

This article was downloaded by:

On: 25 January 2011

Access details: *Access Details: Free Access*

Publisher *Taylor & Francis*

Informa Ltd Registered in England and Wales Registered Number: 1072954 Registered office: Mortimer House, 37-41 Mortimer Street, London W1T 3JH, UK



Separation Science and Technology

Publication details, including instructions for authors and subscription information:

<http://www.informaworld.com/smpp/title~content=t713708471>

MODELING, PARAMETRIC ESTIMATION, AND SENSITIVITY ANALYSIS FOR COPPER ADSORPTION WITH MOSS PACKED-BED

Nabil Abdel-Jabbar^a; Sameer Al-Asheh^a; Belal Hader^a

^a Department of Chemical Engineering, Jordan University of Science and Technology, Irbid, Jordan

Online publication date: 31 October 2001

To cite this Article Abdel-Jabbar, Nabil , Al-Asheh, Sameer and Hader, Belal(2001) 'MODELING, PARAMETRIC ESTIMATION, AND SENSITIVITY ANALYSIS FOR COPPER ADSORPTION WITH MOSS PACKED-BED', Separation Science and Technology, 36: 13, 2811 – 2833

To link to this Article: DOI: 10.1081/SS-100107631

URL: <http://dx.doi.org/10.1081/SS-100107631>

PLEASE SCROLL DOWN FOR ARTICLE

Full terms and conditions of use: <http://www.informaworld.com/terms-and-conditions-of-access.pdf>

This article may be used for research, teaching and private study purposes. Any substantial or systematic reproduction, re-distribution, re-selling, loan or sub-licensing, systematic supply or distribution in any form to anyone is expressly forbidden.

The publisher does not give any warranty express or implied or make any representation that the contents will be complete or accurate or up to date. The accuracy of any instructions, formulae and drug doses should be independently verified with primary sources. The publisher shall not be liable for any loss, actions, claims, proceedings, demand or costs or damages whatsoever or howsoever caused arising directly or indirectly in connection with or arising out of the use of this material.

MODELING, PARAMETRIC ESTIMATION, AND SENSITIVITY ANALYSIS FOR COPPER ADSORPTION WITH MOSS PACKED-BED

**Nabil Abdel-Jabbar,* Sameer Al-Asheh,
and Belal Hader**

Jordan University of Science and Technology,
Department of Chemical Engineering, P.O. Box 3030,
Irbid 22110 Jordan

ABSTRACT

The dynamic behavior of copper adsorption system with a column packed with a biological sorbent moss was predicted successfully with a rigorous dynamic mathematical model. The model considers resistances due to axial dispersion, external film and intraparticle diffusion in addition to the Freundlich equilibrium isotherm. Adsorption parameters must be defined for the mathematical model to be solved. Therefore, a parameter estimation procedure via optimization is presented to simultaneously determine the model parameters and validate the model prediction. A typical range of values was selected for the system parameters, and the system sensitivity to the changes in the parameters was explored. Numerical simulation results are in good agreement with the experimental results at different operating conditions.

*Corresponding author. Fax: +(962)-2-7095018; E-mail: nabilj@just.edu.jo

INTRODUCTION

Adsorption is a separation technique normally used for the removal of pollutants from the environment. The removal of pollutants from the environment is essential due to their diverse deleterious effects. Heavy metals are among those pollutants and several conventional adsorbents, such as activated carbon and ion exchange resins, have been recognized for the removal of these metals from their solutions. Having in mind the high capital and regeneration costs of these materials, researchers were encouraged to look for new sorbents from biological origins. For example, the yeast *Saccharomyces cerevisiae* (1), the algal *Sargassum fluitans* (2), and moss (3) have been used for the removal of heavy metals from aqueous solutions. These biosorbents have the advantages of high metal selectivity, low production cost, and possibility of reutilization.

Often adsorption processes are conducted in columns packed with sorbent. The most important characteristic feature of packed-bed adsorption is the breakthrough curve, which depends on the process operating conditions, such as influent flow rate and concentration. These breakthrough curves determine the effectiveness of the sorbent and the sorption process. They could be obtained using lab-scale experiments. However, for a suitable model that describes the adsorption system, the breakthrough curves can be predicted theoretically without the need to conduct expensive experiments. Mathematical models can also facilitate scaling-up the adsorption process.

Mathematical models describing the adsorption process in packed columns are normally represented by partial differential equations. These models are generally obtained by applying differential material balance to the column and include terms such as axial dispersion, external mass transfer, and intraparticle mass transfer. In general, analytical solutions of these models are difficult to obtain due to their complexity and nonlinearity, but numerical techniques can be used to solve this system (4). Though several approximate analytical solutions can be used to simplify the original complex models (5,6,7), these approximate forms are valid only under certain specified conditions. Model simplifications may lead to inaccurate results; alternatively numerical techniques can be used rigorously to solve the overall unsimplified model.

Relatively recently, considerable advances were addressed in numerical simulations of adsorption systems. These include the implementation of finite difference schemes (4,6,8), the orthogonal collocation method (9,10), and the finite element method (11,12). The finite difference methods are the most widely used due to their simplicity and applicability to most types of differential equations. However, the stability and accuracy of the solution from the finite difference method may be less than in the more complicated schemes, such as the finite element method. The orthogonal collocation method is known to be more accurate than the finite difference especially when a large number of collocation points are



used. However, a large number of collocation points will introduce oscillation and instability problems in addition to more computational cost.

Most of the recent works in solving similar models focused on the development of numerical solutions using model parameters obtained from the literature (4,6,7,13). Others used certain mathematical correlations to evaluate the model parameters (2,14). Other authors evaluated some of the model parameters through reconciliation of the model prediction with experimental results using certain optimization techniques (8,15).

The objective of this work is to rigorously model the packed-bed sorption for the removal of copper using moss. Parametric estimation strategy will be presented to predict the key parameters describing the system under consideration. Sensitivity analysis was employed to investigate the influence of the adsorption parameters on the process behavior. Effects of different operating conditions on the breakthrough curves were considered using theory.

MOSS ADSORPTION SYSTEM

Al-Asheh (3) studied experimentally the continuous adsorption process of copper through a packed-bed of moss. A tubular Plexiglas column that was 20 cm long with a 1.2 cm i.d. and packed with 5 g moss was used to study the concentration profile, i.e. the change in copper concentration along the bed with time. The experiments were carried out under different influent copper concentrations and influent flow rates. Samples were collected from ports located in the column at 4, 8, 12, 16, and 20 cm from the bottom (see Fig. 1). The process continued until the metal concentration from the top of column became the same as the influent concentration. Detailed procedures are presented elsewhere (16).

MATHEMATICAL MODEL

The model equations of the adsorption process describe the spatial and temporal distribution of adsorbate inside the adsorbent particles and in the bulk liquid phase. The main transport mechanisms in the fluid phase are convection due to fluid flow and axial dispersion (diffusion) along the column. Inside the particles, molecules could diffuse into the inner portion either via surface diffusion, pore diffusion, or both. In the present model, resistances due to axial dispersion, external film and intraparticle diffusion were considered. The following assumptions were made in the analysis:

1. Plug flow with constant axial velocity is evident along the column.
2. The temperature is constant throughout the column (298 K).



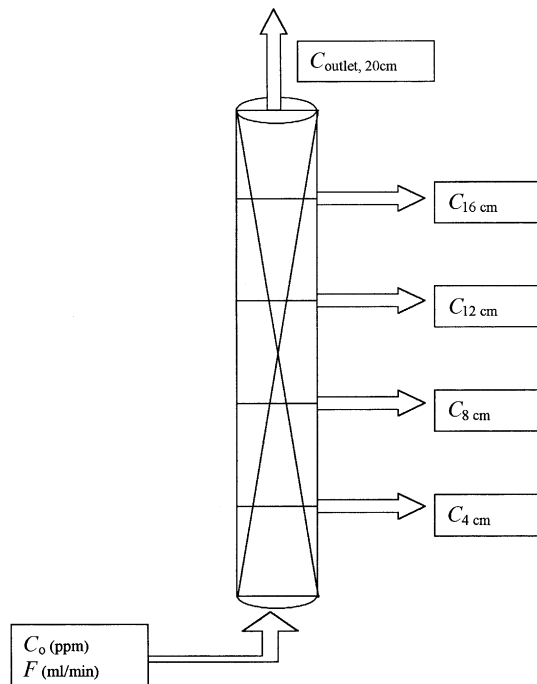


Figure 1. Schematic diagram of the moss adsorption column.

3. The adsorbent particles are spherical.
4. Fick's law of diffusion governs the transport within the adsorbent particles and the axial dispersion in the bulk fluid phase.

Liquid-Phase Dynamics

Based on the above assumptions and using the shell-balance method, we described the mass transport from the flowing fluid phase to the fixed adsorbent by the following differential equation:

$$D_{\text{ax}} \frac{\partial^2 C}{\partial Z^2} - V_Z \frac{\partial C}{\partial Z} = \frac{\partial C}{\partial t} - \frac{1 - \varepsilon}{\varepsilon} \frac{dC_s}{dt} \quad (1)$$

The rate of change of adsorbate concentration on the solid particles can be represented by introducing the mass transfer coefficient (17) where

$$\frac{\partial C_s}{\partial t} = \frac{k_f a}{1 - \varepsilon} (C - C_i) \quad (2)$$



If Eqs. (1) and (2) are combined, the liquid-phase dynamics will be governed by

$$\frac{\partial C}{\partial t} = D_{\text{ax}} \frac{\partial^2 C}{\partial Z^2} - V_Z \frac{\partial C}{\partial Z} - \frac{k_f a}{\varepsilon} (C - C_i) \quad (3)$$

The initial and boundary conditions of the above equation are

$$\text{at } t = 0, \quad 0 \leq Z \leq L; \quad C = 0 \quad (4)$$

$$\text{at } t \geq 0, \quad Z = 0; \quad C = C_o \quad (5)$$

$$\text{at } t \geq 0, \quad Z = L; \quad \frac{\partial C}{\partial Z} = 0 \quad (6)$$

Intraparticle Transport

The description of adsorption dynamics within the solid particles require the unsteady state diffusion equation based on Fick's law. If the particles are solid spheres, a mass balance approach produces the following equation:

$$\frac{\partial q}{\partial t} = \frac{D_e}{r^2} \frac{\partial}{\partial r} \left(r^2 \frac{\partial q}{\partial r} \right) \quad (7)$$

or

$$\frac{\partial q}{\partial t} = D_e \left(\frac{\partial^2 q}{\partial r^2} + \frac{2}{r} \frac{\partial q}{\partial r} \right) \quad (8)$$

The above equation is subjected to the following initial and boundary conditions:

$$\text{at } t = 0, \quad 0 \leq r \leq R_p; \quad q = 0 \quad (9)$$

$$\text{at } t \geq 0, \quad r = 0; \quad \frac{\partial C}{\partial r} = 0 \quad (10)$$

$$\text{at } t \geq 0, \quad r = R_p; \quad D_e \rho_p \frac{\partial q}{\partial r} = k_f (C - C_i) \quad (11)$$

The boundary condition described by Eq. (10) reflects the symmetry of the mass flux at the center of the spherical particle, and the one represented by Eq. (11) is based on the identical mass flux to the particle surface by diffusion through the external liquid film and into the particle.

Equilibrium Isotherm

The equation that describes the equilibrium between copper ions in the solution and that in moss was best represented by the Freundlich isotherm model (3).

$$q_i = K C_i^{1/n} \quad (12)$$



The Freundlich equilibrium equation was used in combination with the system of partial differential equations in the model (Eqs. 3 and 8).

Model Solution

The system of partial differential equations was transformed to a system of ordinary differential equations (ODEs) using the method of lines. Backward difference formulas were used to discretize the first and second partial derivatives in the Z direction. This discretization is justified by the flow pattern of solution, which was assumed to be a plug flow type. However, forward and central difference formulas were used to discretize the first and second partial derivatives in the r direction. The resulting system of ODEs is highly stiff due to the different time scales of the physical parameters. For example, the effective diffusion coefficient is usually in the order of $10^{-12} \text{ cm}^2/\text{s}$ while the axial diffusion coefficient is in the order of $10^{-3} \text{ cm}^2/\text{s}$. This difference causes a large spread in the magnitude of the local eigen values, which may lead to an unstable solution. The system of ordinary differential equations was solved by means of the MATLAB software package using the stiff-suited solver ode23tb.

The method of lines gives discrete solutions of the concentration profiles at different sections along the column. These solutions automatically provide the breakthrough curves at each sampling port (4, 8, 12, 16, and 20 cm) without the need to solve the model for each port individually. This solution method can be used effectively to match the model prediction with the experimental data for the purpose of model verification and parameter estimation. The use of MATLAB facilitated this task because it has readily available ODE solvers and optimization toolboxes.

Estimation of Model Parameters

In this work, the model parameters (effective diffusion coefficient, D_e ; fluid mass transfer coefficients, k_f ; the Freundlich equilibrium constants, $1/n$ and K ; and the specific surface area, a) were estimated through comparisons of model predictions with experimental data. The specific surface area, a , was included in the parameter estimation due to the lack of experimental measurements and inaccurate approximations found in the literature. The axial diffusion coefficient, D_{ax} , has a negligible effect on the copper adsorption by moss; thus, it was evaluated with a theoretical correlation (18).

Parameter estimation via optimization is a computationally intensive task because the model needs to be solved at each iteration for a given set of parameters until a suitable objective function is minimized. The objective function to be



minimized reflects the agreement between the theoretical model prediction and experimental data. The ability to find all model parameters at the same time with reasonable accuracy and without the need for theoretical correlations is the main advantage of the method outlined in this work.

The Objective Function

The objective function was chosen such that the optimization routine minimizes the error between model prediction and experimental data. This objective function is the least square formula based on the sum of absolute errors. The objective function was formulated as follows:

After the ode23tb solver determined the breakthrough curves at the 5 ports (4, 8, 12, 16, and 20 cm), the absolute error (AE) between the experimental and theoretical concentrations was calculated for each data point as a function of time:

$$AE_i = \left| \left(\frac{C_i^{\text{exp}}}{C_o} \right) - \left(\frac{C_i^{\text{theo}}}{C_o} \right) \right|; \quad i = 1, 2, 3, \dots, n \quad (13)$$

where C_i^{exp} is the experimental concentration at time step t_i and C_i^{theo} is the theoretical concentration at time t_i . This produces 5 AE vectors corresponding to each port. Then all of the AEs in each vector are summed together to give the sum of absolute errors (SAE).

$$SAE = \sum_{i=1}^n \left(\left| \left(\frac{C_i^{\text{exp}}}{C_o} \right) - \left(\frac{C_i^{\text{theo}}}{C_o} \right) \right| \right) \quad (14)$$

Each element in the SAE vector is then squared and summed to produce the sum of the squares of errors (SSE). The SSE is then used as the objective function in the optimization routine. The MATLAB optimization routine `constr` is used to optimize the model parameters such that the minimum SSE is obtained.

$$SSE = \sum_{j=1}^5 (SAE_j)^2; \quad j = 1, 2, \dots, 5 \quad (15)$$

Initial Estimate of the Parameters

Several iterations are usually needed to reach convergence in optimization problem solutions. In addition, the result might be sensitive to the initial estimate of the parameters. A good initial guess is essential for the optimization solution because it improves the execution efficiency and can help locate the best minimum in less computational time. The initial values of parameters were calculated using suitable theory correlations or those from related experimental findings found in literature.



Sensitivity Analysis

Sensitivity analysis is based on one-at-a-time parameter perturbation and repeated re-solution of the model (20). For every calculation, one parameter is changed from its baseline value while the other parameters are fixed at their baseline values. Baseline values for the model parameters were obtained from the parametric estimation results. Each parameter was changed from a typical low value to a higher value that includes all of the base values. In this range, the breakthrough curves at the top of the column ($Z = 20$ cm) were predicted by solving the model, and then $t_{0,1}$ was determined.

To quantify the influence of the model parameters on the breakthrough curves, sensitivity analyses were performed at a performance criterion. This criterion was based on the breakthrough time, which is defined as the time when a relative concentration (C/C_o) of 0.1 from the effluent of the column is reached ($Z = 20$ cm) and is designated as $t_{0,1}$ (9). Generally speaking, as $t_{0,1}$ increases, the breakthrough curves become more flattened and the adsorption process is more favorable. In addition, the increase in $t_{0,1}$ indicates that the column can be saturated after a relatively long period of time.

RESULTS AND DISCUSSION

The experimental data used in this work were taken from the previous work of Al-Asheh and Duvnjak (16). The model prediction of breakthrough curves, at different influent concentrations and influent flow rates, was compared with experimental data at identical operating conditions. For each set of operating conditions, the model parameters, effective diffusion coefficient (D_e), fluid mass transfer coefficient (k_f), specific surface area (a), and Freundlich equilibrium isotherm constants ($1/n$ and K), were determined so that the model prediction matched the experimental data. These parameters were also investigated through sensitivity analysis. In addition, the effects of influent concentration (C_o), influent flow rate (F), bed depth (Z), bed void fraction (ε), particle size (d_p), bed diameter (d_b), and axial diffusion coefficient (D_{ax}) on the adsorption process are presented and discussed.

Model Prediction

The experimental data, which were extracted from Al-Asheh (3), covered a reasonable range of operating conditions and was designed for study of the effect of influent concentration, influent flow rate, and bed height on copper adsorption by moss.

Figures 2 and 3 show that model predictions are in good agreement with the experimental data. This agreement can be noticed for most of the cases at each



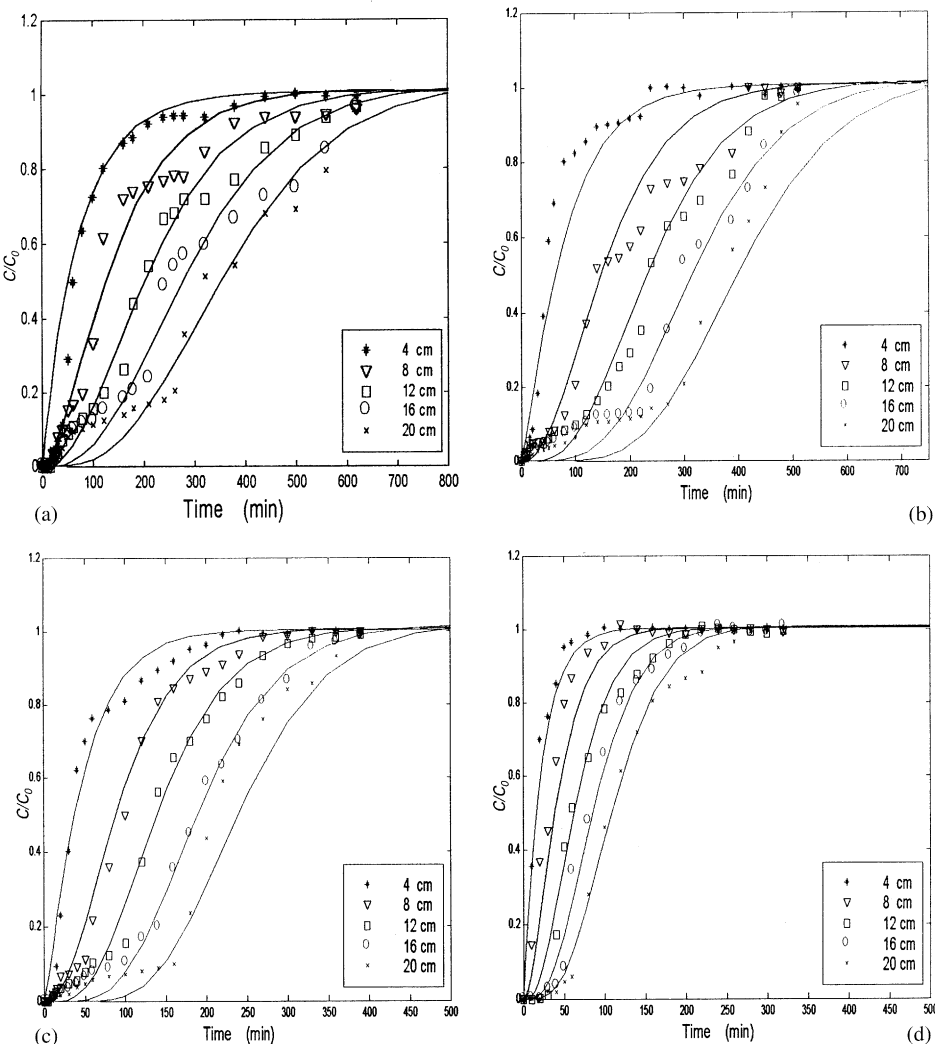


Figure 2. Breakthrough curves for copper sorption by moss-packed bed at different influent copper concentrations. Average flow rate: 8 mL/min; influent copper concentration (ppm): (a) 25, (b) 50, (c) 75, (d) 100. Symbols represent experimental data and solid lines represent model predictions.

port along the column. The agreement between the experimental data and the model prediction implies that the model adequately describes the adsorption behavior in the column. The predicted breakthrough curves are shown to be stable and accurate.



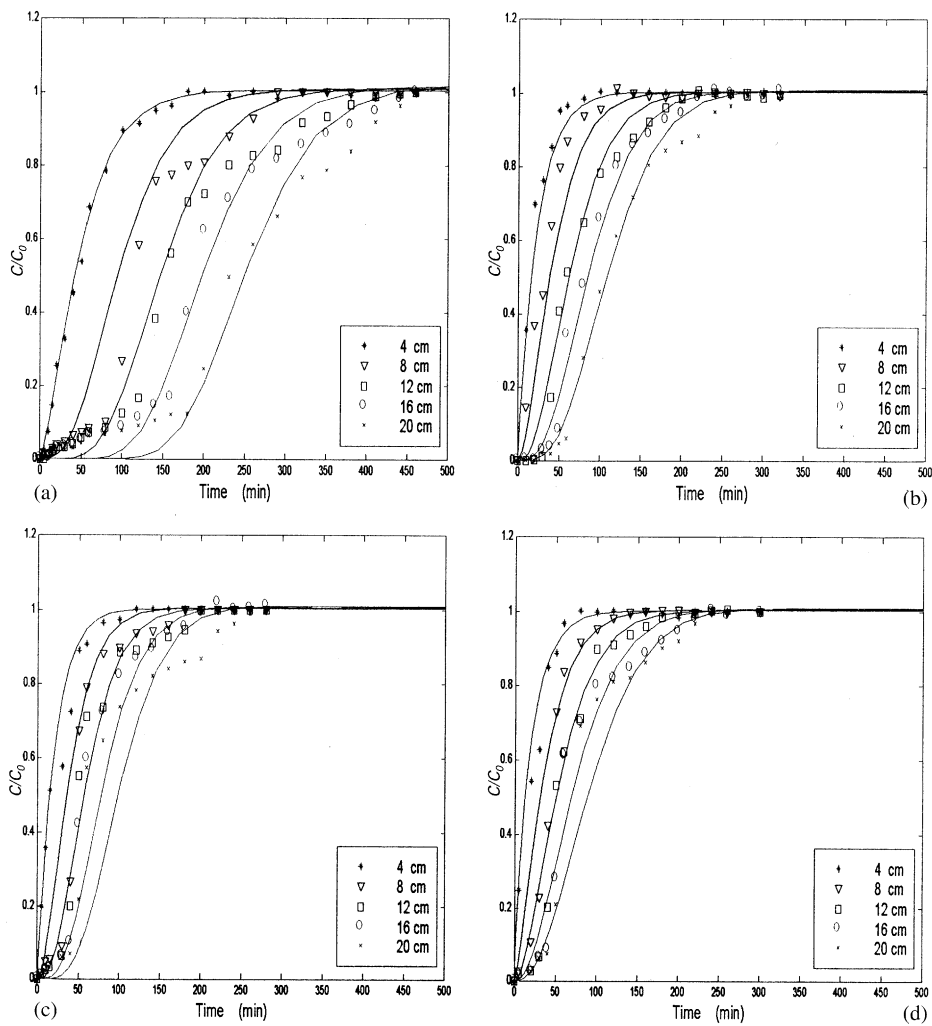


Figure 3. Breakthrough curves for copper sorption by moss-packed bed at different influent flow rates. Influent copper concentration: 100 ppm; influent flow rate (mL/min): (a) 2.5, (b) 8.4, (c) 16.6, (d) 26.0. Symbols represent experimental data and solid lines represent model predictions.

The effect of influent concentrations was investigated at 25, 50, 75, and 100 ppm of copper (Fig. 2). At all port locations, a decrease in the influent concentration resulted in a delay in the breakthrough occurrence; hence, the breakthrough curves are shifted to the right. The shorter time is due to the faster saturation of the mass transfer zone when higher influent concentrations are used.



To determine the effect of the solution flow rate on the performance of the column, experiments were carried out at flow rates of 2.5, 8.4, 16.6, and 26.0 mL/min with an influent copper concentration of 100 ppm (Fig. 3). Larger flow rates resulted in a shorter breakthrough time and a shift of the breakthrough curve to the left. This result was found for each port along the column. With the increase of the influent flow rate, the influent load of copper to the bed will also increase. In addition, the velocity inside the bed will increase causing the fluid mass transfer resistance to be lower. This will cause the column to be saturated faster. Thus, decreasing influent flow rates will favorably increase the breakthrough time as well as the saturation time of the column.

Optimum Model Parameters

The model parameters were estimated through an iterative procedure in which the *ode23tb* routine solved the system of ODEs for each updated set of parameters until the objective function was minimized. The *constr optimization* routine was used to minimize the objective function and to update the values of the parameters until the termination tolerance was satisfied. The estimated model parameters at different operating conditions are presented in Table 1.

Table 1 also shows the sum of the squares of errors (SSE) for each set of operating conditions. The D_e values are in a very small range ($7.1\text{--}9.5 \times 10^{-12}$ cm 2 /s) for all cases. This result indicates that changes in influent concentration and flow rate have a negligible effect on D_e . Therefore, an average D_e value of 8.30×10^{-12} cm 2 /s can be used for all cases. This conclusion is supported by the sensitivity analysis results, as subsequently discussed.

The values of k_f at different influent concentrations up to 75 ppm are very similar; however, the highest value of k_f is at 100 ppm. Therefore, the influent con-

Table 1. Optimum Model Parameters at Different Operating Conditions and the Sum of Squares of Errors for Different Simulations

C_o (ppm)	F (cm 3 /min)	$D_e \times 10^{12}$ (cm 2 /s)	$k_f \times 10^3$ (cm/s)	a (cm 2 /cm 3)	1/n	K (mmol/g)	SSE
25	8.8	7.108	5.373	137.08	1.0263	0.9720	8.438
50	7.8	7.759	5.252	133.24	0.8637	0.9080	8.967
75	7.0	8.326	6.071	134.25	0.8461	0.6864	3.573
100	2.5	8.176	5.692	134.53	0.7110	0.6803	6.803
100	8.4	7.868	7.704	130.13	0.9984	0.387	1.998
100	16.6	9.328	8.465	121.90	0.9497	0.4327	2.958
100	26.0	9.532	8.947	135.21	1.1763	0.4080	3.412

SSE is sum of square errors.



centrations, up to 75 ppm, do not have a significant effect on the mass transfer coefficient, k_f . This result was expected, because the system can be considered diluted. Yet, the increase in influent flow rate resulted in a slight increase in k_f . For example, at a flow rate of 2.5 cm³/min, the estimated k_f value was 5.69×10^{-3} cm/s; however, when the flow rate was increased to 26.0 cm³/min, k_f was 8.95×10^{-3} cm/s. Because increase in the influent flow rate increases the velocity and decreases the film resistance to mass transfer, the mass transfer coefficient is increased.

The specific surface area values were, as expected, relatively constant. Because the same particles were used for all experiments, the average value of 132.3 cm²/cm³ was used as the specific surface area of the bed particles. This value is about 4 times higher than that estimated from the empirical correlation for spherical particles. This difference is justified because the correlation was based on the assumption that the particles are perfect spheres; however, the irregularities in the shape and the high number of pores of the moss particles considerably increase the available specific surface area.

The Freundlich isotherm constants ($1/n$ and K) are in good agreement with the experimental findings (20). These constants can be affected by changes in other experimental conditions, such as temperature and pH, that cause variations at different operating conditions. Al-Asheh (3) showed that slight changes in temperature or pH may considerably affect Freundlich constants, especially the K values. The values $1/n$ are close to 1.0, which indicates that the Freundlich equilibrium isotherm is almost linear. This linearity is due to the relatively low copper concentrations considered in this work.

The SSE was between 1.998 and 8.967. The SSE represents the minimum error between the model prediction and the experimental data. Approximately 95–120 experimental data points were found for all the ports for each case. Figure 4 shows the variations of the SSE for a range of model parameter values at 25-ppm influent copper concentration and 8.8-mL/min influent flow rate. The optimum values for the parameters found from the optimization search gave, at least locally, a minimum value of SSE in the range of operating conditions studied.

SENSITIVITY ANALYSIS

Effect of Effective Diffusion Coefficient (D_e)

Figure 5a shows the relationship between $t_{0.1}$ and D_e of influent concentration 100 ppm and different flow rates (2.5, 8.4, 16.6, and 26.0 mL/min). Obtained from the simulation results, $t_{0.1}$ is insensitive to the changes in D_e over the range studied for all tested flow rates. However, when the flow rate



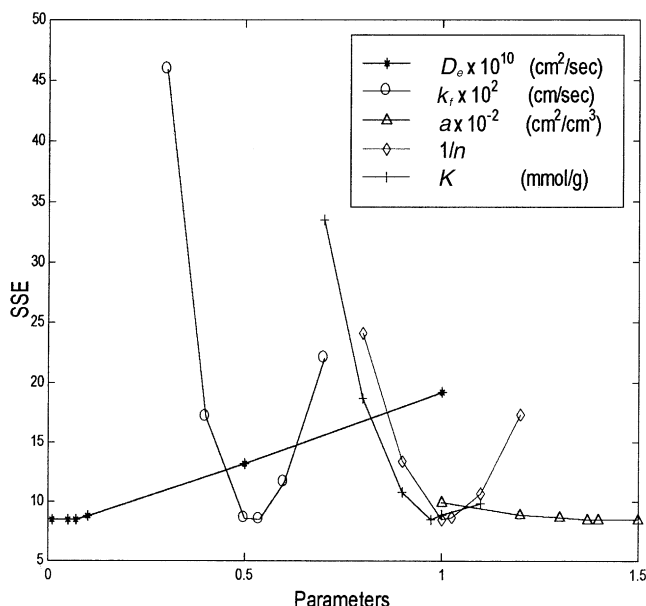


Figure 4. Variations of the SSE for a range of model parameter values at the operating condition of 25-ppm influent copper concentration and 8.8- mL/min influent flow rate.

decreased, $t_{0.1}$ increased, and therefore, the breakthrough curves drifted to the right. Figure 5b shows the relationship between $t_{0.1}$ and D_e at influent concentrations of 25 and 100 ppm and relatively constant influent flow rate. Again, $t_{0.1}$ was insensitive to the changes in D_e over the studied influent concentrations. This insensitivity indicates that the value of D_e is dominated by surface diffusivity and is not influenced by the influent concentration or influent flow rate.

Effect of Mass Transfer Coefficient (k_f)

Figure 6a shows the relationship between $t_{0.1}$ and k_f with influent concentrations of 100 ppm and various flow rates, while Fig. 6b shows this relationship but at copper concentrations of 25 and 100 ppm and average flow rate of 8.2 mL/min. $t_{0.1}$ was sensitive to changes in k_f , especially at low flow rates. As k_f increased, the breakthrough curves became less flattened and $t_{0.1}$ decreased. The increase in k_f results in a decrease in the film mass-transfer resistance, and therefore the particles would be saturated faster. Because at high k_f values the resistance will



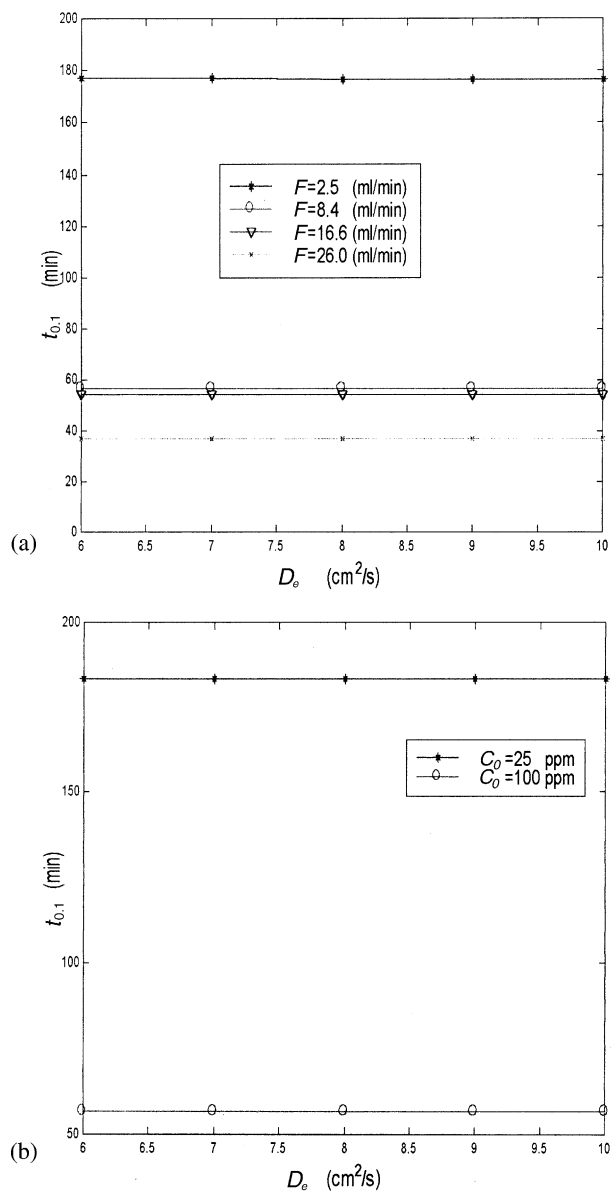


Figure 5. Relationship between $t_{0.1}$ and the effective diffusion coefficient ($D_e \times 10^{12}$) at 100-ppm influent copper concentration and different influent flow rates (a) and at an influent flow rate of 8.2 mL/min and different influent copper concentrations (b).



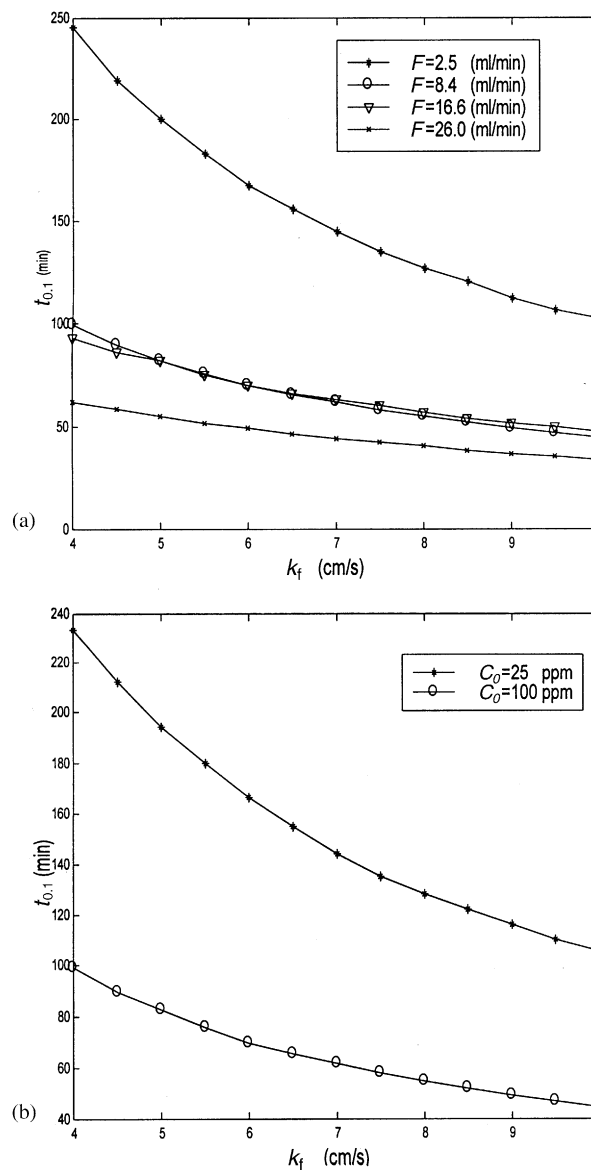


Figure 6. Relationship between $t_{0,1}$ and the mass transfer coefficient ($k_f \times 10^3$) at 100-ppm influent copper concentration and different influent flow rates (a) and at an influent flow rate of 8.2 mL/min and different influent copper concentrations (b).



be smaller and insignificant compared with the high effective diffusion resistance, $t_{0.1}$ is less sensitive to high k_f ranges for all operating conditions.

Effect of Freundlich Isotherm Constants ($1/n$ and K)

Figure 7a presents the relationship between $t_{0.1}$ and $1/n$ at different flow rates and influent concentration of 100 ppm, while Fig. 7b presents the relationship at different influent copper concentrations (25 and 100 ppm) and average flow rate of 8.2 mL/min. Both figures indicate that $t_{0.1}$ is slightly sensitive to variations in $1/n$, especially at the high $1/n$ values. However, the $1/n$ values are in the range of 0.7–1.0, which have slight influence on $t_{0.1}$.

Figure 8 presents the relation between $t_{0.1}$ and the Freundlich constant K . $t_{0.1}$ is very sensitive to changes in the K values and linearly increased with the increase in the K values. As K increased the capacity of moss particles to adsorb more copper ions increased, and therefore, the breakthrough curves were shifted to the right and resulted in longer periods for saturation to occur. To increase the capacity of adsorption and to improve the adsorption process, one can change the pH or temperature such that the Freundlich isotherm constant K increases.

Effect of Axial Diffusion Coefficient (D_{ax})

To study the effect of axial diffusion coefficient (D_{ax}) on the performance of the model, the value of D_{ax} was changed 10-times lower and 10-times higher than the base value (2.571×10^{-3} cm 2 /s). This was done for the case of 25-ppm influent copper concentration and 8.8-mL/min influent flow rate. The breakthrough curves were almost identical as the lines coincided over each other for all values of D_{ax} tested at all ports. This result indicates that these breakthrough curves are insensitive to the variations in D_{ax} . This insensitivity suggests that the transport of copper ions via axial dispersion is negligible compared to that achieved with the convective transport.

Effect of Bed Depth (Z)

Figures 2 and 3 show the breakthrough curves at the different ports along the column (4, 8, 12, 16, and 20 cm). For all cases, as the bed height increase, the breakthrough time and the time for total saturation increased. In other words, when the bed depth increases the breakthrough curve will favorably drift to the right due to the increased available mass-transfer zone for the adsorption process. The relationship between $t_{0.1}$ and bed depth is almost linear for all flow rates tested.



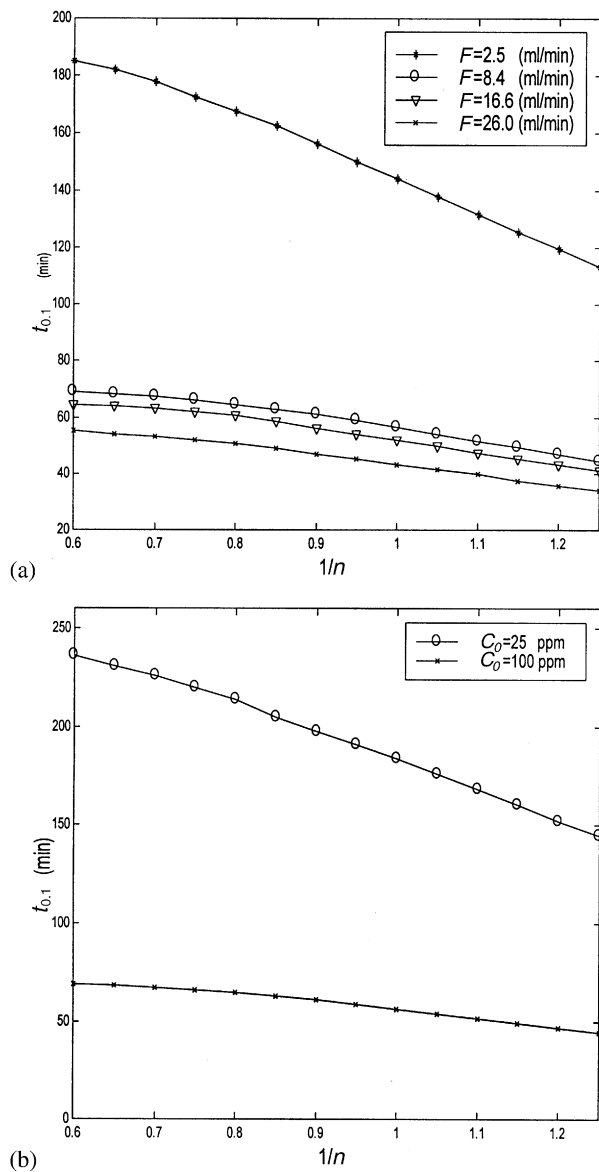


Figure 7. Sensitivity of $t_{0.1}$ to the Freundlich isotherm constant ($1/n$) at 100-ppm influent copper concentration and different influent flow rates (a) and at an average influent flow rate of 8.2 mL/min and different influent copper concentrations (b).



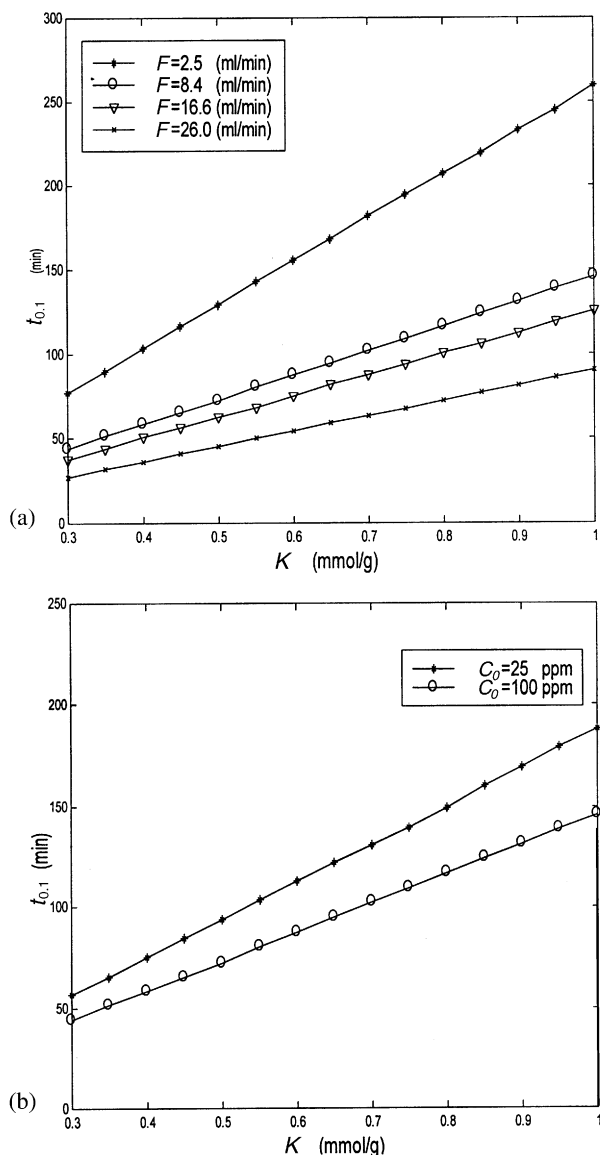


Figure 8. Sensitivity of $t_{0.1}$ to the Freundlich isotherm constant (K) at 100-ppm influent copper concentration and different influent flow rates (a) and at an average influent flow rate of 8.2 mL/min and different influent copper concentrations (b).



Effect of Bed Void Fraction (ε)

The model was used to study the effect of bed void fraction (ε) on the copper adsorption process by moss. In all experiments the bed void fraction was very high ($\varepsilon = 0.79$), which means that most of the bed was empty. This condition was due to the fluffy nature of the sorbent. We wanted to know if variations in ε would improve the performance of the column. For this purpose, ε was varied from a high packing degree at $\varepsilon = 0.3$ to a low degree at $\varepsilon = 0.79$ at different operating conditions. Results of these simulations are shown in Fig. 9. The decrease in ε (i.e. the increase in the packing degree) caused a significant increase in the breakthrough time and a favorable shift to the right for the breakthrough curves. For example, $t_{0.1}$ was increased from about 180 to 600 minutes when ε was decreased from 0.79 to 0.3 (Fig. 9). When the void fraction is decreased, the column becomes more packed with moss particles, which increases the column capacity for copper ions. In addition, the additional moss would decrease the effect of channelling so that the contact of the fluid with the solid surface increases. Also, as the void fraction decreases, the height of transfer units in the bed decreases and the number of transfer units increases, which will lead to a better mass-transfer operation. However, this favorable behavior could be affected by a higher pressure

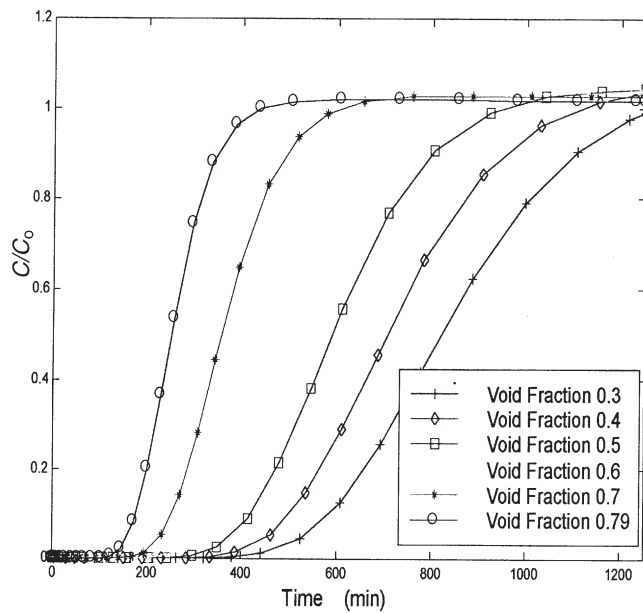


Figure 9. Effect of bed void fraction (ε) on the breakthrough curves. Influent copper concentration: 100 ppm; influent flow rate: 2.5 mL/min; $Z = 20$ cm.



drop across the bed when a high packing material is used. For this reason, more experiments are needed to find the best void fraction of the bed for an improved adsorption process.

Effect of Particle Size (d_p)

The effect of moss particles size on the adsorption process was also studied through the use of the model prediction of breakthrough curves. In the experimental work, only one particle size was considered ($d_p \approx 0.036$ cm). In the present study, d_p was changed from 0.01 cm to 0.1 cm and breakthrough curves were obtained (Fig. 10). The decrease in particle size significantly improved the performance of the column. For example, as d_p decreased from 0.036 to 0.01 cm, $t_{0.1}$ increased from approximately 180 to 600 minutes (Fig. 10). The decrease in particle size significantly increases the available area for mass transfer, and therefore, increases the adsorption capacity of the bed. However, decreasing the particle size may cause particle coagulation problems, which may lead to unfavorable operation. Therefore, the optimum particle size must be carefully determined for the adsorption process.

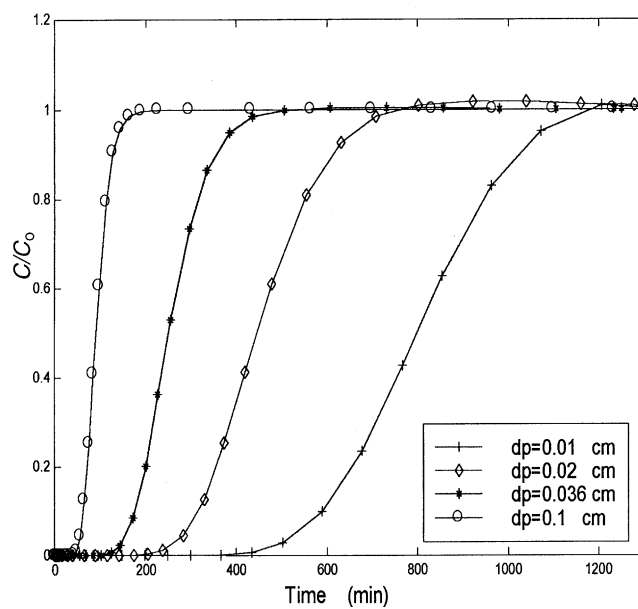


Figure 10. Effect of particles size (d_p) on breakthrough curves. Influent copper concentration: 100 ppm; influent flow rate: 2.5 mL/min; $Z = 20$ cm.



CONCLUSIONS

In the light of the results and discussion, the following conclusions can be drawn from this work:

1. The model used is shown to be successful in predicting the behavior of copper adsorption using the moss-packed bed. The model prediction of the breakthrough curves is in good agreement with the experimental data at different operating conditions.
2. Breakthrough time increases with the decrease in influent concentration (C_o), influent flow rate (F), moss particles size (d_p), bed void fraction (ε), and with the increase in bed height (Z).
3. The model is sensitive to changes in mass transfer coefficient (k_f), Freundlich equilibrium isotherm constant (K), moss particles size (d_p), and bed void fraction (ε).
4. Influent copper concentration and influent flow rate have negligible effects on the effective diffusion coefficient (D_e). An average D_e value of $8.30 \times 10^{-12} \text{ cm}^2/\text{s}$ can be used for all simulations without affecting the model prediction.
5. The effect of axial dispersion coefficient (D_{ax}) on the copper adsorption of moss-packed bed is negligible.

NOMENCLATURE

a	specific surface area (cm^2/cm^3)
b	Langmuir constant (L/mmol)
C	metal concentration in the fluid phase (mmol/L)
C_i	interfacial metal concentration (mmol/L)
C_o	influent metal concentration (mmol/L)
C_s	metal concentration in the solid phase (mmol/L)
D	diffusion coefficient in water (cm^2/s)
D_{ax}	axial dispersion coefficient (cm^2/s)
D_e	effective diffusion coefficient in the particles (cm^2/s)
d_b	bed diameter (cm)
d_p	particle diameter (cm)
F	influent flow rate (mL/min)
K	Freundlich constant related to sorbent capacity (mmol/g)
k_f	fluid mass-transfer coefficient (cm/s)
L	length of the packed bed (cm)
$1/n$	Freundlich constant related to sorbent intensity
q	amount of adsorbed metal (mmol/g)
r	radial direction in the solid particles (cm)



R_p	radius of solid particles (cm)
$t_{0.1}$	time at which C/C_o reaches 0.1 (minutes)
t^{exp}	experimental time steps (minutes)
t^i	time step (min)
t^{theo}	theoretical time steps from the ODE solver (minutes)
V_z	interstitial fluid velocity inside the bed (cm/s)
Z	distance from the bottom of the bed (cm)
ε	bed void fraction
ρ_p	density of solid particles (g/cm^3)

ACKNOWLEDGMENT

The financial support provided by the Deanship of Research at Jordan University of Science and Technology under Grout 198/99 is gratefully acknowledged.

REFERENCES

1. Volesky, B.; May, H.; Holan, Z. Cadmium Biosorption by *Saccharomyces Cerevisiae*. *Biotech. Bioeng.* **1993**, *41* (11), 826.
2. Yang, J.; Volesky, B. Intraparticle Diffusivity of Cd Ions in a New Biosorbent Material. *J. Chem. Technol. Biotech.* **1996**, *66* (4), 355.
3. Al-Asheh, S. Sorption of Heavy Metals by Biological Materials. Ph.D. diss., University of Ottawa, Canada, 1997.
4. Sun, L.; Meunier, F. An Improved Finite Difference Method for Fixed-Bed Multicomponent Sorption. *AIChE J.* **1991**, *37* (6), 244.
5. Lai, C.; Tan, C. Approximate Models for the Nonlinear Adsorption in Packed-Bed Adsorber. *AIChE J.* **1991**, *37* (3), 461.
6. Smith, E. Modified Solution of Homogeneous Surface Diffusion Model for Adsorption. *J. Environ. Eng.* **1991**, *117* (3), 321.
7. Xiu, G.; Nitta, T. Breakthrough Curves for Fixed-Bed Adsorbers: Quasi-Lognormal Distribution Approximation. *AIChE J.* **1997**, *43* (4), 979.
8. Eichenmuller, B.; Bunke, G.; Behrend, K.; Buchholz, R.; Gotz, P. Adsorption of Acenaphthene on Porous Organic Polymers. *J. Environ. Eng.* **1997**, *123* (9), 836.
9. Ma, Z.; Guiochon, G. Application of Orthogonal Collocation Finite Element in the Simulation of Nonlinear Chromatography. *Comp. Chem. Eng.* **1991**, *15* (5), 415.
10. Roy, D.; Wang, G.; Adrian, D. A Simplified Solution Technique for Carbon Adsorption Model. *Wat. Res.* **1993**, *27* (6), 1033.
11. Hossain, M.; Young, D. Finite Element Modeling of Single-Solute Acti-



vated Carbon Adsorption. *J. Environ. Eng.* **1992**, *118* (2), 39.

12. Speitel, G.; Zhu, X. Sensitivity Analysis of Biodegradation Adsorption Models. *J. Environ. Eng.* **1990**, *116* (1), 33.

13. Sun, W.; Costa, C. Fast Method for Solving Nonequilibrium Fixed-Bed Adsorption Models with Variable Velocity and Linear Isotherm. *Comp. Chem. Eng.* **1992**, *16* (6), 535.

14. Carlsson, F.; Axelsson, A.; Zacchi, G. Mathematical Modeling and Parametric Studies of Affinity Chromatography. *Comp. Chem. Eng.* **1994**, *18* (suppl), S657.

15. Traegner, U.; Sudan, M. Parameter Evaluation for Carbon Adsorption. *J. Environ. Eng.* **1989**, *115* (1), 109.

16. Al-Asheh, S.; Duvnjak, Z. Continuous Recovery of Copper Ions from Aqueous Solutions using a Moss-Packed Column. *J. Haz. Mat.* **1998**, *2* (1), 57.

17. Hines, A.; Maddox, R. *Mass Transfer Fundamentals and Applications*. Prentice-Hall: Englewood Cliffs, NJ, 1984.

18. Wakao, N.; Funazkri, T. Effect of Fluid Dispersion Coefficients on Particle-to-Fluid Mass Transfer Coefficients in Packed-Beds. *Chem. Eng. Sci.* **1978**, *33* (5), 1375.

19. Leis, J.; Kramer, M. Sensitivity Analysis of Systems of Differential and Algebraic Equations. *Comp. Chemical Eng.* **1985**, *9* (1), 93.

20. McCabe, W.; Smith, J.; Harriott, P. *Unit Operations of Chemical Engineering*, Fifth Ed.; McGraw-Hill: New York, 1993; 692–705.

Received March 2000

Revised November 2000



Request Permission or Order Reprints Instantly!

Interested in copying and sharing this article? In most cases, U.S. Copyright Law requires that you get permission from the article's rightsholder before using copyrighted content.

All information and materials found in this article, including but not limited to text, trademarks, patents, logos, graphics and images (the "Materials"), are the copyrighted works and other forms of intellectual property of Marcel Dekker, Inc., or its licensors. All rights not expressly granted are reserved.

Get permission to lawfully reproduce and distribute the Materials or order reprints quickly and painlessly. Simply click on the "Request Permission/Reprints Here" link below and follow the instructions. Visit the [U.S. Copyright Office](#) for information on Fair Use limitations of U.S. copyright law. Please refer to The Association of American Publishers' (AAP) website for guidelines on [Fair Use in the Classroom](#).

The Materials are for your personal use only and cannot be reformatted, reposted, resold or distributed by electronic means or otherwise without permission from Marcel Dekker, Inc. Marcel Dekker, Inc. grants you the limited right to display the Materials only on your personal computer or personal wireless device, and to copy and download single copies of such Materials provided that any copyright, trademark or other notice appearing on such Materials is also retained by, displayed, copied or downloaded as part of the Materials and is not removed or obscured, and provided you do not edit, modify, alter or enhance the Materials. Please refer to our [Website User Agreement](#) for more details.

Order now!

Reprints of this article can also be ordered at
<http://www.dekker.com/servlet/product/DOI/101081SS100107631>